Limiting pump intensity for sulfur-doped gallium selenide crystals

2014 Laser Phys. Lett. 11 055401

(http://iopscience.iop.org/1612-202X/11/5/055401)

IOP Publishing | Astro Ltd
Laser Physics Letters
Laser Phys. Lett. **11** (2014) 055401 (6pp)
doi:10.1088/1612-2011/11/5/055401

Letters

Limiting pump intensity for sulfur-doped gallium selenide crystals

J Guo[1], D-J Li[1], J-J Xie[1], L-M Zhang[1], Z-S Feng[2, 3], Yu M Andreev[4, 5], K A Kokh[6, 7], G V Lanskii[4, 5], A I Potekaev[5], A V Shaiduko[4, 5] and V A Svetlichnyi[5]

[1] State Key Laboratory of Laser Interaction with Matter, Changchun Institute of Optics, Fine Mechanics and Physics of Chinese Academy of Sciences, 3888 Dongnanhu Rd., Changchun 130033, People's Republic of China
[2] Key Laboratory of Coherent Light and Atomic and Molecular Spectroscopy of Ministry of Education and College of Physics, Jilin University, 2519 Jie-Fang Rd., Changchun 130023, People's Republic of China
[3] Aviation University of Air Force, 2222 Nanhu Rd., Changchun 130022, People's Republic of China
[4] Institute of Monitoring of Climatic and Ecological Systems, Siberian Branch of Russian Academy of Sciences, 10/3 Academical Ave., Tomsk 634055, Russia
[5] Siberian Physical-Technical Institute of Tomsk State University, 1 Novosobornaya Sq., Tomsk 634050, Russia
[6] Institute of Geology and Mineralogy, Siberian Branch of Russian Academy of Sciences, 3 Koptyuga Ave., Novosibirsk 630090, Russia
[7] Novosibirsk State University, 2 Pirogova Str., Novosibirsk 630090, Russia

E-mail: yuandreev@imces.ru

Received 12 February 2014
Accepted for publication 19 February 2014
Published 17 March 2014

Abstract
High optical quality undoped and sulfur-doped gallium selenide crystals were grown from melts by the modified vertical Bridgman method. Detailed study of the damage produced under femtosecond pulse exposure has shown that evaluation of the damage threshold by visual control is unfounded. Black matter spots produced on crystal surfaces do not noticeably decrease either its transparency or its frequency conversion efficiency as opposed to real damage identified as caked well-cohesive gallium structures. For the first time it was demonstrated that optimally sulfur-doped gallium selenide crystal possesses the highest resistivity to optical emission (about four times higher in comparison with undoped gallium selenide).

Keywords: frequency conversion, nonlinear optical crystals, doped gallium selenide, damage threshold

(Some figures may appear in colour only in the online journal)

1. Introduction

Layered ε-polytype gallium selenide (GaSe) is one of the best nonlinear optical materials for frequency conversion within an extremely wide spectral range from the near IR (0.7895 μm) [1] through to the mid- [2] and far IR [3, 4], up to 5640 μm [5]. GaSe possesses attractive optical properties such as a high second order nonlinear coefficient ($d_{22} = 54$ pm/V at 10.6 μm [2] and 24.3 pm/V at 300 μm [6]), huge birefringence (0.375 at 10.6 μm [2] and 0.79 at 300 μm [7]), and a high optical damage threshold [8], similar to that of the so-called 'mid-IR standard nonlinear crystal' $ZnGeP_2$ [9].

On the other hand, GaSe demonstrates very weak hardness (≈0 in Mohs' scale) [2] and clearly marked cleavage along c-cut growth planes, which makes cutting and polishing optical faces difficult [10]. Another unfavorable effect of the layered structure is the existence of four (ε, δ, β and γ) polytypes, all of which may be found in a single GaSe crystal. Besides, due to specific features of the growth process, GaSe is characterized by a relatively high absorption coefficient $\alpha \geqslant 0.1$–$0.2\,\mathrm{cm}^{-1}$

governed by the point defects (mainly Ga vacancies) and micro-defects (stacking faults, second phase inclusions, local slicing-offs, bulbs, dislocations, broken layers) [10–12]. These disadvantages limit frequency conversion efficiency and hold back the out-of-lab applications of GaSe.

2. Gallium selenide modification

Fortunately, GaSe well incorporates different isovalent impurities that can significantly strengthen the structure and improve the optical quality at appropriately chosen concentrations, whilst somewhat modifying other physical properties responsible for frequency conversion efficiency. This occurs mainly due to a decrease in the number of point defects by substitution with impurity atoms [13] that in turn leads to a reduction in the number of stacking faults. The most impressive modification of GaSe physical properties was demonstrated by sulfur-doping (GaSe : S) [14]. The significant shift of the short-wave edge decreases linear [15] and nonlinear [16] optical losses for near IR pump. Regulation of the dispersion properties through the control of doping concentration allows optimization of phase matching conditions [15] and reduces refractivity [17]. As a result, operation of the GaSe : S(10 mass%) optical parametric generators (OPG), oscillators (OPO) and amplifiers (OPA) under Nd : YAG laser pump has demonstrated about three times better performance than that of undoped GaSe under identical pump intensities, mainly due to lower two-photon absorption [18–20]. Operation of the GaSe : S(2 mass%) difference frequency generation (DFG) by a two-frequency (1.064 and 1080 μm) Nd : YAG laser system showed 1.45 times higher efficiency in THz generation due to the decreased optical losses and refractivity [17]. On the other hand, heavy S-doping proportionally reduces GaSe nonlinearity [14, 16, 19, 21], thus decreasing potential frequency conversion efficiency. However, 2.4 times higher mid-IR efficiency of the second harmonic generation (SHG) has been reported [15] in optimally doped GaSe : S(2–3 mass%) crystal. Increased efficiency was attributed to the full set of modified physical properties including an increased (but not defined quantitatively) damage threshold [15].

3. Damage threshold

Previous studies of the damage threshold and limitations on pump pulse intensity were carried out mainly on undoped GaSe [8, 10, 22–24]. GaSe resistance to continuous wave (CW) pump was studied only for CO_2 (9.67 μm) [25] and Nd : YVO_4 (1.064 μm) [18] lasers. Available data on the GaSe : S damage threshold are incomplete and inconsistent. In accordance with [26], under femtosecond (fs) pulse exposure all GaSe:S were demonstrated 10–15% lower damage threshold (identified visually by plasma observation) than that of undoped GaSe, independent of the pump wavelength within the 2.12–2.9 μm range. Under 120 ns CO_2 laser (10.6 μm) and 250 ns Er^{3+}:YSGG laser (2.94 μm) pulsed exposure, GaSe : S(2–9 mass%), demonstrated a 1.15–1.3 times higher damage threshold than that of GaSe [27]. The advantage for GaSe : S(10 mass%) was 1.44 and 1.67 times higher under exposure by 14 ns pulses and CW emission from the Nd : YVO_4 laser, respectively [18]. The advantage was up to 1.63 times higher under exposure to CO_2 laser pulses with a 50 ns leading peak and intense microsecond 'tail' [28]. The advantage grows up to 1.5–1.8 times for GaSe : S(2 mass%) under exposure of CO_2 laser pulses with a 120 ns leading peak and short (1 μs) low-intensity 'tail' [21].

It should be mentioned that in the above cited studies, principal factors governing the damage threshold such as the optical quality of the crystals and spectral parameters, pulse duration, and time shape-form of the pump pulses, varied significantly from experiment to experiment. Besides, different criteria for the damage threshold determination were applied: (1) visually observed plasma emission [22], (2) barely distinguishable by eye disturbance (a crack and/or matter caked after melting) [18, 28] or (3) cracking leading to a wave front distortion [18]. Gray tracks in GaSe : S(10 mass%) were observed at an intensity level roughly corresponding to 80% of the damage threshold but they did not limit frequency conversion efficiency [18]. It was proposed that gray tracks are not related to surface damage or cracking. It is evident that increased damage threshold can be exploited for further improvement in the frequency conversion efficiency by increasing the pump intensity. Detailed knowledge of damage threshold depending on S-doping allows frequency conversion efficiency to be improved by appropriate choice of the doping concentration.

In this study, we report a detailed investigation of the impact of fs pulses on undoped GaSe in comparison with GaSe : S(0.5, 1, 2, 3, 7, 10 mass%) grown from the melts. The general aim was also to find the dependence of the damage threshold on the S-doping level and to formulate a suitable criterion for determining the limiting pump intensity.

4. Crystal growth

Synthesis of stoichiometric GaSe and GaSe : S(0.5, 1, 2, 3, 7, 10 mass%) was performed in a single-zone horizontal furnace by the modified technology according to the steps described in detail in [12]. Synthesized material fills ⩾95% of the ampoule volume, thus limiting interaction with the rest gases and improving optical quality.

Synthesized polycrystalline material was reloaded into the growth ampoules of 22 mm in diameter with a pyrolytic carbon layer deposited onto the inner surface. The sealed ampoules were heated to 1000 °C and maintained for several days in order to dissolve the dopant (S). The last step was a slow unseeded crystallization by the modified vertical Bridgman technique in a single-zone furnace with a heat field rotation for efficient charge mixing [29]. Each ampoule was mechanically pulled down at a speed of 5 mm/day through the temperature gradient of ≈15 K/cm. Low-speed crystal growth with efficient charge mixing yields highly uniform optical quality crystals. A very small segregation was observed in the end section of the grown ingots.

The samples for the study were cleaved along the growth layers from nose sections of as-grown ingots; no additional

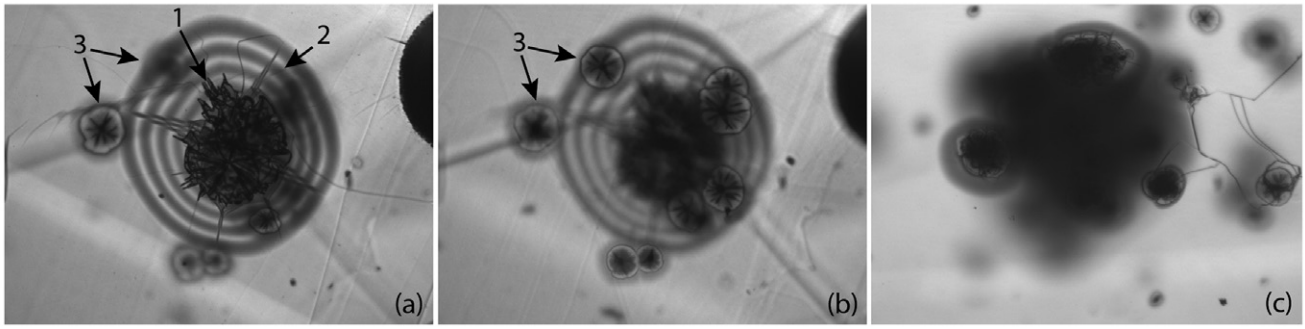

Figure 1. View of the same local point of a crystal surface with transmission microscope at two (*a*), (*b*) different focus depths: 1 is damage at a position of a sliced-off region (in the center), 2 (rings) is an interference pattern, 3 are mini local sliced-off regions (white color strips around micro-precipitations); (*c*) black matter formation on the local surface section after exposure with increased fs pulse intensity.

treatment or surface polishing was made. A few crystals containing micro-defects were specially selected and studied in comparison.

5. Facility and measurement method

Hexagonal (ε-GaSe-type) structure of the grown GaSe : S crystals was verified by XRD and TEM observations, and by the nonlinear method [30]. Electron probe micro-analyses (EPMA) was used for measurement of Ga and Se contents with a JXA-8800M (JEOL) device. The atomic emission spectrometry method was used to measure the S-content with an inductively coupled plasma optical emission (ICP-OE) spectrometer iCAP 6500 (Thermo Scientific): detection limit $\approx 10^{-4}$. UV–visible transparency spectra were recorded by a Cary 100 Scan (Varian Inc.) spectrophotometer: operation wavelength range 190–900 nm, spectral resolution 0.2–4 nm, wavelength deviation ± 1 nm. Mid-IR optical spectra were recorded by a FTIR Nicolet 6700 spectrometer: 11000–375 cm^{-1}, spectral resolution 0.09 cm^{-1}. Low quality crystals containing micro-defects were selected and studied for comparison with a transmission Micmed-6 (Russia) microscope (magnification from $\times 4$ to $\times 100$). The crystal surfaces were also studied by an atomic force microscope (AFM) Solver HV (NT MDT, Zelenograd, Russia).

The pump source employed in the experiment was a Ti : sapphire laser system. It included a Nd : YLF laser Verdi-5V (Coherent) supplied with a BBO SHG pumping a Ti:sapphire mode-locked master laser Mira 900-B (Coherent). Approximately 100 fs (FWHM) master laser pulses were applied to pump a Ti : sapphire OPA Legend Elite (Coherent) operating at 0.8 μm. In turn, frequency doubled output of the OPA was used to pump in parallel two tunable Ti : sapphire travelling wave generators (OPG) TOPAS-C (Coherent) emitting from 60 to 90 fs (FWHM) pulses, dependence on the output wavelength, at a repetition rate of 1 kHz. The OPG operation ranges were: 1.1–1.6 μm (signal band) and 1.6–2.9 μm (idler band). To limit two-photon absorption, operation at 2 μm was chosen. The average power of the pump beam was of 0.5 ± 0.005 W. Changeable pyroelectric detectors: a Fieldmaster (Coherent) with a sensitive head OP-2 Vis (Coherent) and a FieldMaxII (Coherent) with a sensitive head LM-10 HTD (Coherent) were used, respectively, to measure the low power reference and the transmitted beams. The pulse amplitudes were recorded by a TDS3052 (Tektronix) oscilloscope.

The measurements were performed at room temperature. In accordance with the measurement procedure used, the pump beams were focused into GaSe by a ZnSe lens (f = 405 mm). The pump intensity was controlled by crystal translation towards the focal plane. The crystal was installed on a high-precision ($\pm 5\,\mu$m) 500-mm translation stage PSA300-11-X (Zolix, China). The beam intensity I_d on the crystal face was estimated by the relation

$$I_d = \frac{2E}{\pi\omega_d^2}\int_0^\infty \frac{\psi(t)}{\psi_{\max}}\,\mathrm{d}t,$$

E is the pulse energy, and $\psi(t)/\psi_{\max}$ is the normalized time pulse shape-form. The beam radius on the crystal face ω_d was estimated by the relation:

$$\omega_d = \omega_{02}\sqrt{1+\left(\frac{f-L_d}{\pi\omega_{02}^2}\right)^2},$$

L_d is the distance to the lens center, $\omega_{02} = \lambda f/(\pi\omega_{01})$ is the Gaussian beam radius in the focus and ω_{01} is the beam radius (6 mm) on the lens input, λ is the emission wavelength [22]. Two criteria were used in determining the damage threshold: visual observation of the produced defects, or plasma and a decrease in the transmitted power to a pre-selected level.

6. Visual observations

Several types of damage caused by the presence of micro defects were observed by the transmission microscope after exposure by fs pulses (figure 1).

At first, damage was produced at the position of the micro precipitations on the crystal surfaces. Subsequently they appeared at the positions of local sliced-off regions and micro precipitations in the crystal bulk along the beam propagation trace. This fact was established by varying the focus depths of the transmission microscope (figures 1(*a*) and (*b*)). With increasing pump intensity, the black colored matter that originates around micro defects spread further, forming overlapping black spots (figure 1(*c*)). At pump intensities over $\geqslant 200$ MW/cm^2 onto a defect-free surface section, a uniform

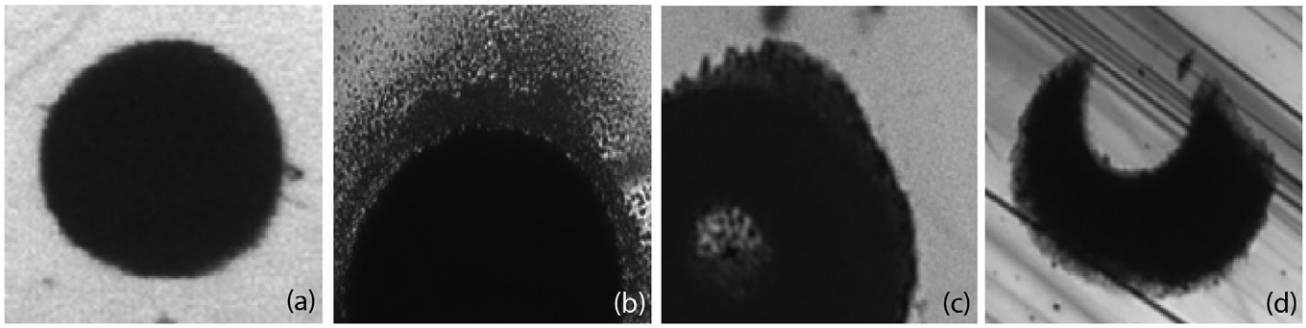

Figure 2. Evolution of the black spot structure under exposure to fs pulses: (*a*) uniform black matter spot formed on a defect-free surface section, (*b*) ejection of diffuse black matter from the spot, (*b*) a crater creation (bottom left), (*c*) the crater with completely ejected matter in the center; the average spot diameter is ≈350 μm.

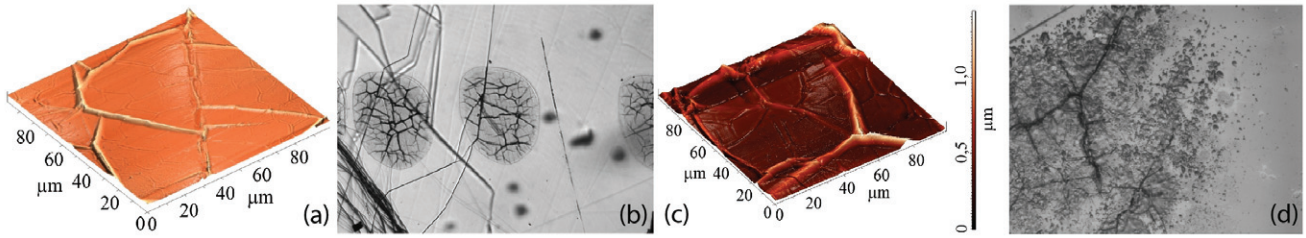

Figure 3. Third stage evolutions of the damage spot: (*a*) an AFM image of a high quality GaSe crystal surface after exposure to sub-TW/cm^2 pump intensity; (*b*) a view of two damage spots on the crystal surface with broken layers, recorded by the transmission microscope; (*c*) an AFM image of a high quality GaSe crystal surface after exposure with 2 TW/cm^2 pump intensity; (*d*) a view of a damage spot on the crystal surface with broken layers after exposure with ≈4 TW/cm^2 pump intensity, recorded by the transmission microscope. (*a*) and (*b*) are in pseudo colors; (*c*) insets are depth scale.

black matter spot emerged (figure 2(*a*)). It grew continuously in diameter with increasing pump intensity, showing some ejection of black matter. With a further increase of the pump intensity, stronger ejection of the diffused black matter from the spot was observed (figure 2(*b*)), resulting in crater creation (figure 2(*c*)). At intensities of a few hundred MW/cm^2, the bottom of the crater appeared clear of the black matter due to ejection, showing undisturbed boundaries of the broken layers (figure 2(*d*)). It was determined by AFM that the layer thickness of the black matter spot is extremely ($\leqslant 1\,\mu$m) thin.

The next stage of the damage spot transformation was observed under exposure to sub- and TW/cm^2 pump intensities. At this stage heavy (takyr-type) deformation of the thin upper layer was observed (figures 3(*a*) and (*b*)) that seems to be caused by both electrostriction and thermal strike effects. Micro images recorded with the AFM showed that the thickness of the damage spots was still on sub-micrometer scale (figure 3(*c*)) and was nearly linearly increasing with the pump intensity. On the takyr-type spot some nanosized solidified Ga protuberances were observed after exposure to the first pulses. Images recorded with the transmission microscope revealed a field of solidificated nanosized Ga particles (figure 3(*d*)) produced under pump intensities of a few TW/cm^2.

7. Results and discussion

Chemical analysis revealed that Ga and Se content of GaSe crystals was well within the homogeneity range; Se content was about 1 at% lower than Ga content [31]. Real S-doping concentrations for crystals grown from the melts GaSe : S(0.5, 1, 2, 3, 7, 10 mass%) were determined as GaSe : S(0.46, 0.95, 1.93, 2.93, 6.91, 9.94 mass%). To avoid confusion, we will hereinafter label the grown crystals in accordance with the growth melt compositions. X-ray and TEM observations verified the hexagonal structure of all grown crystals to be similar to undoped ε-GaSe. The absorption coefficient for the grown crystals was determined as below 0.1 cm^{-1} at the maximal transparency ranges, which is at least 2–3 times lower than that of crystals grown by conventional technology.

Readily removable black matter produced by exposure to a few hundred MW/cm^2 fs pulses was identified by x-ray micro-analysis as a mixture of amorphous selenium (0.02–0.1 mass%), and selenium, sulfur and gallium oxides. It can be proposed that the color of this matter is caused by the black color of amorphous Se. The absorption coefficient (α) for amorphous Se is up to 10^6 cm^{-1} in the visible range and about 5×10^4 cm^{-1} at 0.8 μm, decreasing abruptly at longer wavelengths [32]. From these data, sub-micrometer thickness l_s of the black matter and selenium content in the spot, it can be estimated as the spot's absorptivity $A=\alpha\cdot\ l_s\ \cdot k$, $0.02\leqslant k\leqslant 0.1$. It can be significantly large in the visible range but negligible at wavelength $\geqslant 0.8\,\mu$m. Accordingly, the black matter can be easily identified by observation with naked eyes, but still be weakly attenuating at wavelengths $\geqslant 0.8\,\mu$m. Hence, the visual criterion of the crystal damage threshold does not provide a consistent determination for practical purposes, at least for undoped and S-doped GaSe.

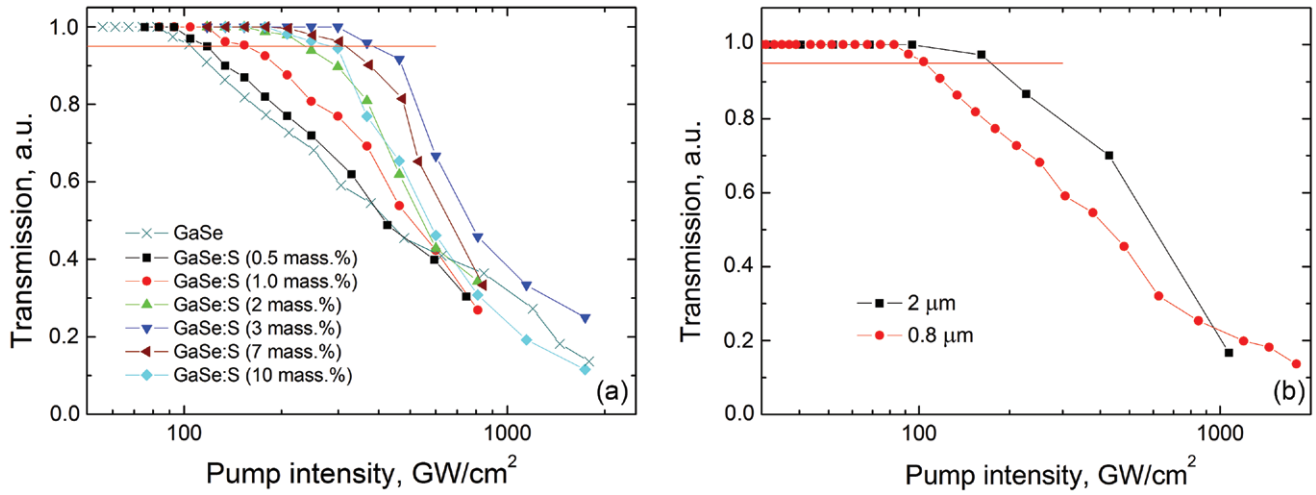

Figure 4. GaSe : S(0.5, 1, 2, 3, 7, 10 mass%) transparencies under exposure to 0.8 μm fs pulse pumping.

It was verified that prolonged exposure by fs pulses of a few hundred MW/cm^2 eventually leads to the formation of a caked Ga structure that is well-cohesive with the crystal surface, is not transparent, and represents real damage. Strongly attenuating cohesive layers with black matter inclusion were also found in the GaSe bulk along the pump beam trace. The black matter spot produced on the crystal surfaces under exposure with sub-TW/cm^2 intensity possessed a non-flat (takyr-type) surface but the same chemical composition as identified above. A non-flat surface structure leads to noticeably (not excessively) decreased transparency, but the rapidly emerging caked Ga structure was not transparent. It should be noted there is no reason to apply exposure of such high intensity or prolonged time as to produce real damage. This is because a dramatic decrease in the transparency and potential frequency conversion efficiency occurs at much lower intensities and shorter exposure times. It was ascertained that dependence of the transparency decrease on pump intensity is most important in determining the maximum possible limit of pump intensity. The transparency drop $\leqslant$0.1 versus pump intensity at 0.8 μm is shown in figure 4.

Specific positions and features of the curves plotted in figure 4(*a*) were well reproducible measurement to measurement. In this figure, it is seen that the highest pump intensity was reached for GaSe : S(3 mass.%). On the other hand, this particular crystal is known as the optimally S-doped GaSe crystal that possesses the best optical quality [15, 26]. Thus, it can be concluded that the optimally doped crystal also possesses the highest resistivity to optical irradiation damage.

In figure 4(*a*) it is also seen that transparency decrease of GaSe : S occurs with noticeably higher gradient than that of undoped GaSe, indicating a different physical origin of the attenuation processes. It leads us to propose the difference in the nonlinear (multiphoton) absorption coefficients as a physical origin for that. Measurement results depicted in figure 4(*b*) confirm this suggestion. In this figure it is seen that changing the pump wavelength from 0.8 to 2 μm (thus excluding two-photon absorption because the short-wave edge of GaSe is at 0.62 μm [10]) leads to $\approx$1.8-fold increase in the pump intensity limit at the fixed transparency magnitude of 0.95.

It is most significant that the dependence of the crystal transparency on pump intensity is multiply reversible. Transparency decline down to the magnitude of $\approx$0.1 under crystal exposure to increasing pump intensity is reversed when pump intensity is again decreased. In other words, if the pump intensity is decreased, the transparency is restored time and again following the same dependency curve. The reversibility demonstrates the absence of real crystal damages in spite of the unavoidable black matter emerging when transparency decreases below the magnitude of 0.4. It confirms once again the inconsistency of the visual criterion in determining the damage threshold, at least for undoped and S-doped GaSe. In our opinion, the best criterion for the determination of the pump intensity limit is the decline in the transparency as a function of pump intensity such that the potential efficiency of the parametric frequency conversion process being considered decreases to an acceptable level. For example, in figure 4 transparency decline down to the magnitude of 0.95 is assumed. The maximum advantage in the pump intensity limit relative to undoped GaSe crystal possessed by the GaSe : S(3 mass.%) crystal is $\approx$4 (figure 4(*a*)), if transparency reduction down to 0.9 is accepted. This result is in good agreement with the majority of known data on the damage threshold and advantage in frequency conversion efficiency of IR nano- and picosecond pulses [18, 21, 27, 28].

8. Conclusion

The modified Bridgman method with heat field rotation for efficient melt mixing was employed to grow uniform ε-polytype undoped GaSe and GaSe : S(0.5, 1, 2, 3, 7, 10 mass.%) crystals, whose real compositions were identified as GaSe : S(0.46, 0.95, 1.93, 2.93, 6.91, 9.94 mass.%). Grown crystals were characterized by a 2–3 times lower optical absorption coefficient compared with crystals grown by the conventional Bridgman technology. It was established that the visual criterion in determining the crystal damage threshold produces inconsistent results, because observation of the black matter damage spots on crystal surfaces does not noticeably decrease either transparency or frequency

conversion efficiency. Real damage was identified as caked well-cohesive Ga structures. It was shown that there can be no reason to apply pumping at such high intensity or long exposure time that would lead to real damages, because a dramatic decrease in the transparency and potential frequency conversion efficiency occurs at much lower intensities and shorter exposure times. Measurement results confirm that nonlinear absorption is a key physical cause for that. For the first time it was demonstrated that optimally sulfur-doped GaSe : S(3 mass.%) crystal possesses the highest resistivity to optical emission that is ≈4 times higher than that of undoped GaSe.

Acknowledgments

This work is partially supported by RFBR Projects, No.12-02-33174.

References

[1] Kador L, Haarer D, Allakhverdiev K and Salaev E 1996 *Appl. Phys. Lett.* **69** 731–3
[2] Dmitriev V G, Gurzadyan G G and Nikogosyan D N 1999 *Handbook for Nonlinear Optical Crystal* 3rd edn, vol 64 (Berlin: Springer) p 414
[3] Dexeimer U L (ed) 2008 *Terahertz Spectroscopy: Principles and Applications* (Boca Raton, FL: CRC Press) p 360
[4] Shi W and Ding Y J 2004 *Appl. Phys. Lett.* **84** 1635–7
[5] Ding Y J and Shi W 2006 *Laser Phys.* **16** 562–70
[6] Tochitsky Ya S, Sung C, Trubnick S E, Joshi C and Vodopyanov K L 2007 *J. Opt. Soc. Am.* B **24** 2509–16
[7] Nazarov M M, Shkurinov A P, Angeluts A A and Sapozhnikov D A 2009 *Radiophys. Quantum Electron.* **52** 536–45
[8] Vodopyanov K L, Kulevskii L A, Voevodin V G, Gribenyukov A I, Allakhverdiev K R and Kerimov T A 1991 *Opt. Commun.* **83** 322–6
[9] Schunemann P 1999 *Laser Focus World* **35** 85–90
[10] Fernelius N C 1994 *Prog. Cryst. Growth Charact.* **28** 275–353
[11] Gouskov A, Camassel J and Gouskov L 1982 *Prog. Cryst. Growth Charact. Mater.* **5** 323–413
[12] Kokh K A, Andreev Yu M, Svetlichnyi V A, Lanskii G V and Kokh A E 2011 *Cryst. Res. Technol.* **46** 327–30
[13] Rak Zs, Mahanti S D, Mandal K C and Fernelius N C 2010 *Phys. Rev.* B **82** 155–203
[14] Allakhverdiev K R, Guliev R I, Salaev Yu E and Smirnov V V 1982 *Sov. J. Quantum Electron.* **12** 947–8
[15] Zhang H-Z *et al* 2008 *Opt. Express* **16** 9951–7
[16] Marchev G, Tyazhev A, Panyutin V, Petrov V, Noack F, Miyata K and Griepentrog M 2011 *Proc. SPIE* **7917** 79171G
[17] Huang J, Huang Z, Tong J, Ouyang C, Chu J, Andreev Yu, Kokh K, Lanskii G and Shaiduko A 2013 *Appl. Phys. Lett.* **103** 81104
[18] Petrov V, Panyutin V L, Tyazhev A, Marchev G, Zagumennyi A I, Rotermund F, Noack F, Miyata K, Iskhakova L D and Zerrouk A F 2011 *Laser Phys.* **21** 774–81
[19] Miyata K, Marchev G, Tyazhev A, Panyutin V and Petrov V 2011 *Opt. Lett.* **36** 1785–7
[20] Miyata K, Marchev G, Tyazhev A, Panyutin V and Petrov V 2011 *CLEO: Science and Innovations (Baltimore, Maryland, 1–6 May 2011)* CTuD2
[21] Zhang Y-F *et al* 2011 *Opt. Commun.* **284** 1677–81
[22] Andreev Yu M, Badikov V V, Voevodin V G, Geiko L G, Geiko P P, Ivashenko M V, Karapuzikov A I and Sherstov I V 2001 *Quantuna Electron.* **31** 1075–8
[23] Vodopyanov K L, Mirov S B, Voevodin V G and Shunemann P G 1998 *Opt. Commun.* **155** 47–50
[24] Vodopyanov K L 1993 *J. Opt. Soc. Am.* **10** 1723–9
[25] Singh N B, Suhre D R, Rosch W, Meyer R, Marable M, Fernelius N C, Hopkins F K, Zelmon D E and Narayanan R 1999 *J. Cryst. Growth* **198** 588–92
[26] Feng Z-S *et al* 2012 *Appl. Phys.* B **108** 545–52
[27] Wu F-G, Andreev Yu M, Lanskii G V, Atuchin V V, Gavrilova T A and Sarkisov S Yu 2008 *Proc. 9th Int. Conf. on Modification of Materials with Particle Beams and Plasma Flows (Tomsk, Russia, 21–26 September 2008)* pp 257–60
[28] Telminov A E, Sitnikov A G, Panchenko A N, Genin D E, Sarkisov S Yu, Beremaya S A, Korotchenko Z V and Vavilin E V 2010 *Proc. 10th Int. Conf. on Modification of Materials with Particle Beams and Plasma Flows (Tomsk, Russia, 19–24 September 2010)* pp 323–4
[29] Kokh K A, Popov V N, Kokh A E, Krasin B A and Nepomnyaschikh A I 2007 *J. Cryst. Growth* **303** 253–7
[30] Andreev Yu M, Kokh K A, Lanskii G V and Morozov A N 2011 *J. Cryst. Growth* **318** 1164–6
[31] Shtanov V I, Komov A A, Tamm M E, Atrashenko D V and Zlomanov V P 1998 *Dokl. Chem.* **361** 140 (Engl. transl.) Shtanov V I, Komov A A, Tamm M E, Atrashenko D V and Zlomanov V P 1998 *Dokl. Akad. Nauk*. **361** (in Russian)
[32] Vasko A 1965 *Czech. J. Phys.* B **15** 170–7